COASTAL WETLANDS

Monitoring the Spatial and Interannual Dynamic of Zostera noltei

Salma Benmokhtar[1] · Marc Robin[2] · Mohamed Maanan[2] · Soilam Boutoumit[1] · Bouabid Badaoui[1] · Hocein Bazairi[1,3]

Abstract

Seagrass is a vital structural and functional element of the marine environment worldwide and is highly valued for its ecological benefits. Monitoring the evolution of the seagrass habitat is essential to understand how this coastal ecosystem changes, and to develop good environmental management practices. For the present study, two remote sensing methods were used to map and monitor *Zostera noltei* Hornemann, 1832 (*Z. noltei*), in the Merja Zerga lagoon from 2010 to 2020. These methods which are the random forest algorithm and the object-oriented classification, were convenient to provide significant results. The first approach employed Sentinel-2 images from 2018 to 2020, which were used to extract information on changes in *Z. noltei* (commonly called dwarf eelgrass) distribution and aboveground biomass estimation. The second involved three orthophotography (orthophoto) mosaics from the years 2010, 2016, and 2018, which were analyzed to map the distribution of the species. It was revealed that *Z. noltei* coverage has increased by 212 ha since 2010, with most of the growth occurring in the center and upstream part of the lagoon. The mean aboveground biomass of dwarf eelgrass in the lagoon was 78.5 DW/m² in 2018, 92.6 DW/m² in 2019, and 115.2 g DW/m² in 2020. The approach used in this study has provided important insights into the dynamic and mean biomass of *Z. noltei* in the Merja Zerga lagoon. It is therefore a valuable, non-destructive method that uses freely-available Sentinel-2 satellite data.

Keywords *Zostera noltei* biomass and mapping · Remote sensing · Orthophoto mosaics and Sentinel-2 satellite data · RF algorithm and OBIA

Introduction

Seagrass is one of the most valuable coastal ecosystems, sustaining a diverse variety of ecologically and economically important marine species (Zulkifli et al. 2021). Vegetated coastal ecosystems, particularly seagrass meadows, are also highly productive and have an extraordinary capacity for carbon dioxide (CO_2) sequestration (Orth et al. 2006; Serrano et al. 2019). The dwarf eelgrass *Zostera noltei* Hornemann, 1832 (*Z. noltei*) is one of the most common intertidal seagrass species representing the land-sea interface (Short and Coles 2001). It extends from Mauritania to southern Norway and the Kattegat in the eastern Atlantic, and is found in the Mediterranean, the Black Sea, the Sea of Azov, the Caspian Sea, the Aral Sea, and the Canary Islands (Green and Short 2003; Diekmann et al. 2010). *Z. noltei* beds provide an extended juvenile habitat for some of the most important species in the food web, and can contribute quantitatively to the function of tidal flats (Polte et al. 2005). Although the International Union for the Conservation of Nature (IUCN) lists *Z. noltei* as a species of little concern, the overall population is said to be falling. The species is particularly sensitive to anthropogenic pressures and climate-change-related impacts in semi-enclosed coastal environments (Cabaço et al. 2011). For example, sea water temperature and sea level rise (SLR) are two pressures that hinder the state, composition, and evolution of the areas occupied by *Z. noltei*, changing it from homogeneous sectors to sparse, patchy

✉ Salma Benmokhtar
  salma_benmokhtar@um5.ac.ma

1 Faculty of Sciences, Department of Biology, Laboratory of Biodiversity, Ecology and Genome, Mohammed V University in Rabat, B.P. 1014 RP, 4 Avenue Ibn Battouta, Rabat 10000, Morocco

2 Institute of Geography, University of Nantes, Nantes 44035, France

3 Natural Sciences and Environment Research Hub, University of Gibraltar, Europa Point Campus, Gibraltar

spots (Short and Neckles 1999; Chust et al. 2011; Dalloyau 2020).

In Morocco, this species is the main type of seagrass in the Atlantic semi-enclosed coastal systems (SECSs): the Merja Zerga, Sidi Moussa, Oualidia, and Khnifiss lagoons and the bay of Dakhla, which are all Ramsar sites. Many authors have demonstrated the significant contribution that *Z. noltei* makes to the biological, ecological, and environmental value of these protected yet vulnerable areas (Hammada 2007; Maanan et al. 2013; Boutahar et al. 2019; Bououarour et al. 2021).

Several authors have effectively assessed spatial distribution and spatio-temporal changes in seagrass ecosystems using remote sensing data, one of the most widespread techniques in this research field (Short and Coles 2001; Hossain et al. 2015; Hossain and Hashim 2019; Rende et al. 2020). The characteristics of the habitats have been assessed using aerial photos (Ferguson et al. 1993; Kirkman 1996; Kendrick et al. 2002), satellite optical images and airborne sensors (Phinn et al. 2008; Lyons et al. 2011, 2013; Pu and Bell 2013; Kovacs et al. 2018; Topouzelis et al. 2018; Benmokhtar et al. 2021), and more recently drone imagery (Duffy et al. 2018). Many recent studies have also demonstrated how to map seagrass carbon stores using multispectral imaging and deep learning algorithms (Hossain et al. 2015; Misbari and Hashim 2016; Tamondong et al. 2018; Pham et al. 2019a; Ha et al. 2021; Stankovic et al. 2021).

This ecosystem mapping now requires updating with an approach that can be easily implemented for long-term monitoring. Among all studies monitoring *Z. noltei* beds in Morocco using remote sensing, Benmokhtar et al. (2021) was the first attempt of its kind to map these beds and estimate their biomass in Merja Zerga lagoon using a random forest algorithm on a SPOT 7 satellite image. For this study, an expansion of Benmokhtar et al. (2021) study, the aim was first to assess the consistency of Sentinel-2 images and random forest classification in mapping *Z. noltei* beds in Merja Zerga lagoon, and thus estimating its aboveground biomass (referred to simply as 'biomass' in the rest of the article). Its second objective was to detect annual changes in the extent of the *Z. noltei* in Merja Zerga lagoon using another approach - an object-based classification method (OBIA) - applied to two orthophoto mosaics.

Study Site and Methods

Merja Zerga Lagoon

The Merja Zerga lagoon is an elliptical-shaped coastal lagoon between 0 and 2 m deep (average depth 50 cm) (Kraiem et al. 2001; Labbardi et al. 2005). It occupies an area of about 30 km². The water temperature ranges between

27° and 28 °C in summer, and 13° and 15 °C in winter (Bazaïri et al. 2003). Merja Zerga lagoon is a Ramsar wetland, the most northerly wetland on the Atlantic coast of Morocco, located 120 km north of Rabat, between 34°47′ and 34°53′ north and 6°13′ and 6°19′ west (Fig. 1). It is influenced by Atlantic tidal rhythms with a range of around 1.4 m, increasing to 3.6 m during the spring tide and dropping to 0.80 m during the neap tide (Alaoui et al. 2010). Atlantic tidal water is the main source of the volume of water in the lagoon (Roelfsema et al. 2009), but it also receives fresh water from the artificial Canal de Nador located at its southern end, incorporating drainage water, and the Drader River at its northern end.

The local communities use the Merja Zerga lagoon resources for many activities, such as tourism, cattle raising and fisheries (Alaoui et al. 2010). Anthropogenic pressures of this type have increased over the last 25 years with a 150% rise in population around the lagoon (Maanan et al. 2013).

The Merja Zerga lagoon is also an important ecological resource and has been part of the CASSARINA and MEL-MARINA projects in the last 20 years (Flower and Thompson 2008). These two projects integrated many studies based on observation and fieldwork that were carried out in the Merja Zerga lagoon, mainly in terms of hydrological characteristics, environmental changes, and contaminants in sediment, plankton and fish fauna (Kraiem et al. 2001; Appleby et al. 2001; Thompson et al. 2009).

Satellite Images and Orthophotos

Studies of the interannual dynamics of seagrass must take into consideration seasonal variability, hence only images taken in the same season can be consistently analyzed without unintentionally producing temporal bias (Roelfsema et al. 2013). The Sentinel-2 images that were analyzed for this study (Table 1) were thus obtained during the summer (August - September), i.e. the period of maximum growth for *Z. noltei* and also the period when the spatial variability of the Normalized Vegetation Index (NDVI) is at its lowest (Zoffoli et al. 2020).

All images were acquired at low tide during a high coefficient tide, to include a large proportion of the intertidal seagrass meadows. The three Sentinel-2 images were downloaded from the US Geological Survey Earth Explorer data portal (https://earthexplorer.usgs.gov/) (Table 1), already pre-processed at level 1 C (with pixels at the top of atmosphere reflectance values) and geocoded to World Geodetic System 1984 datum EPSG CODE 4326. An atmospheric correction to surface reflectance values was required before analysis.

The two satellites, Sentinel-2 A and Sentinel-2B, produce images at a high spatial resolution spanning between 10 and 60 m every five days. Each satellite carries a single
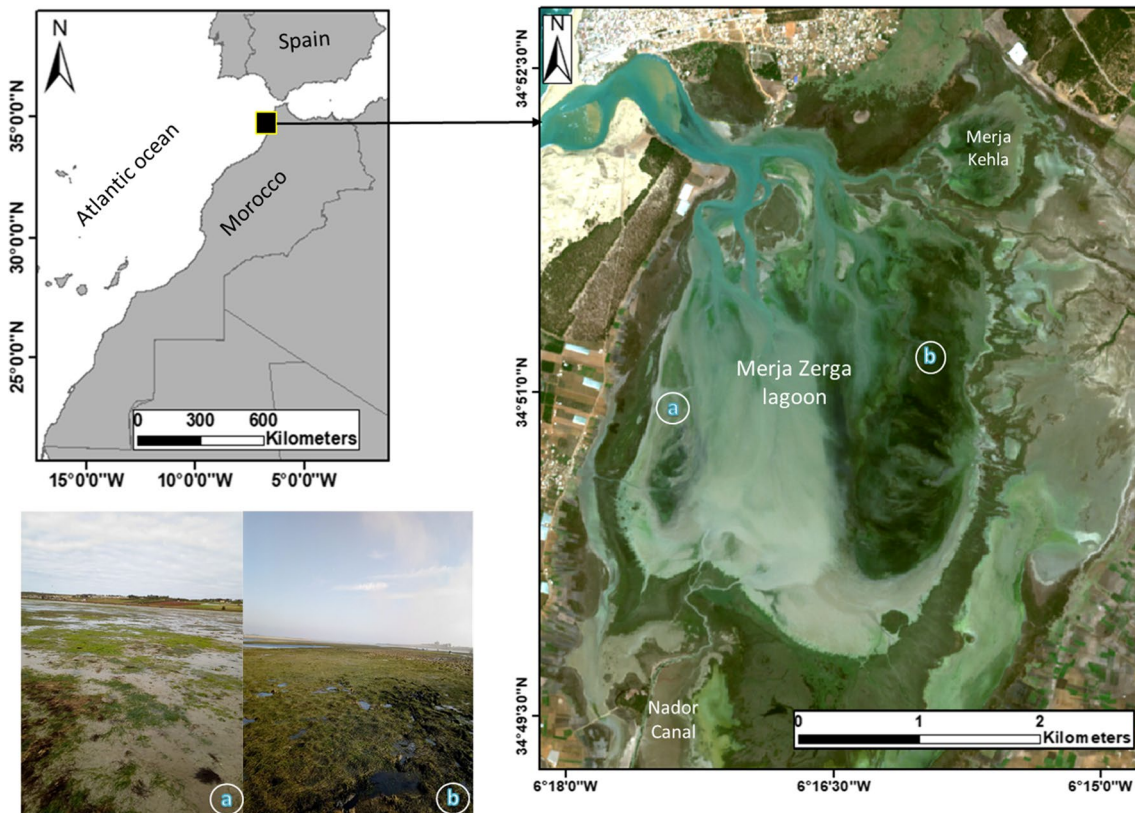
Fig. 1 Geographic location of the Merja Zerga lagoon with field views of sparse (**a**) and (**b**) dense beds of *Z. noltei*. (Source satellite image: Sentinel-2 satellite image 09.28.2020)

multispectral instrument with 13 spectral bands within visible, Near-Infrared, and shortwave infrared spectra, some of which are specially adapted to detect vegetation. In this study we used the three bands in the visible range (Band 2, Band 3, Band 4) and the Near-Infrared band (Band 8) (Table 2).

In addition, to detect the interannual variability of *Z. noltei* bed distribution in the Merja Zerga lagoon, three mosaics of orthophotographs dated 2010, 2016 and 2018 (Fig. 2) with a respective spatial resolution of 1.5 m and 1.3 m were obtained from the National Agency for Land Conservation, Cadaster and Cartography (ANCFCC), the mosaics comprising 4 orthophotographs for 2010, 16 orthophotographs for 2016 and 2 orthophotographs for 2018. Based on these mosaics,

a detailed habitat map of the Merja Zerga lagoon was produced for each year.

The three Sentinel-2 images and three mosaics were classified to produce maps of eight habitat types in this lagoon. The classification process applied to the Sentinel-2 imagery for mapping the Merja Zerga lagoon ecosystems is presented in Fig. 2. The pre-processing and processing steps for the Sentinel-2 imagery used in this study were carried out using the following software packages: R (R Core Team 2019), Orfeo Toolbox in QGIS, ArcGIS, eCognition.

Image Processing

Two classification methods were used to map the *Z. noltei* beds in the Merja Zerga lagoon: a supervised classification

Table 1 Characteristics of the three Sentinel-2 images analyzed in this study

| Acquisition date	Level	Spatial resolution (m)	Time of acquisition (U.T)	Low tide level (m)	Time of Low tide (U.T + 1)	Tidal coefficient	Cloud %
09.29.2018	L1C	10	11 :10	0.7	12 :04	74	0.7
08.20.2019	L1C	10	11 :13	0.8	12 :20	66	0.01
09.28.2020	L1C	10	11 :09	1.1	07 :39	70	0.0

Table 2 Spectral and spatial characteristics of Sentinel-2 bands in the visible range (Band 2, Band 3, Band 4) and the Near-Infrared band (Band 8)

Spectral band	Center wavelength (nm)	Band width (nm)	Spatial resolution (m)
Band 2	490	65	10
Band 3	560	35	10
Band 4	665	30	10
Band 8	842	115	10

approach was used with the Sentinel-2 images, with a random forest (RF) algorithm (this approach was inspired from Benmokhtar et al. 2021 study) and an object-based classification (OBIA) carried out on the mosaics (Fig. 3). The Sentinel-2 images used were first atmospherically corrected using the Dark Object Subtraction 1 (DOS1) available in the Semi-Automatic Classification Plugin version 7.9.10 Matera in QGIS software v. 3.16.4. The DOS1 turns satellite images from top-of-atmosphere (TOA) reflectance into surface reflectance (Prieto-Amparan et al. 2018). The method is fully automatic and requires only the properties of the image with no additional input settings. The visible and Near-Infrared bands of the Sentinel-2 images were used, and seventeen indices were calculated (Table 3). To improve classification accuracy, the resulting layers for each Sentinel-2 image were then stacked on a 21-band image (the four Sentinel-2 raw bands and seventeen calculated indices) and used later in the RF model using the R software.

The classifications were carried out by manual digitization using ArcGIS 10.40. software, with training polygons consisting of eight land cover classes. Each land cover was based on personal field knowledge: shallow water, sand, mud, terrestrial plants, algae, mixed algae and dwarf eelgrass, submerged dwarf eelgrass, emergent dwarf eelgrass. The total number of polygons used to classify each image was 100 for 09.29.2018 Sentinel-2 satellite images,
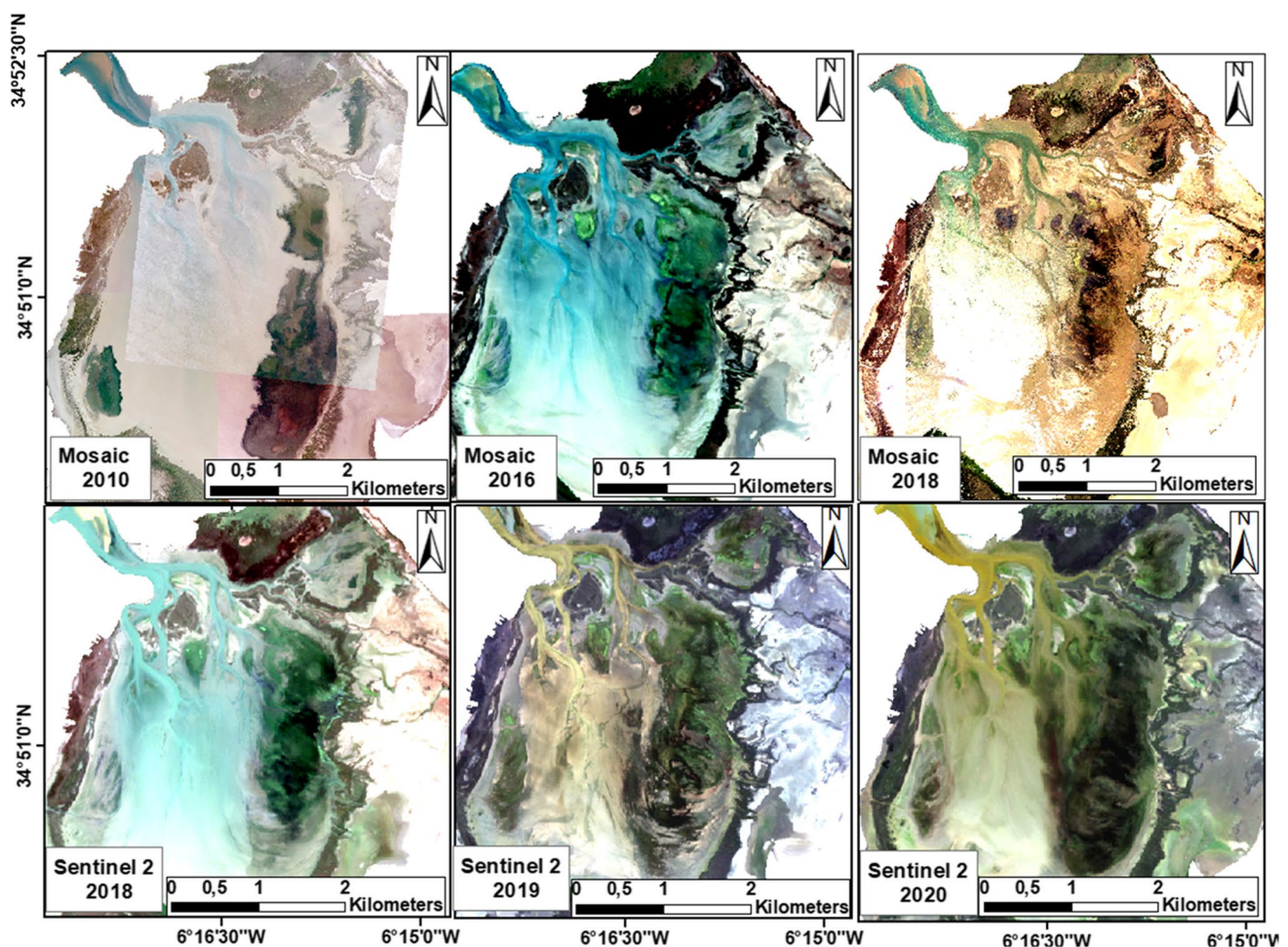
Fig. 2 Mosaics of orthophotographs of the Merja Zerga lagoon: 2010, 2016 and 2018; the Sentinel-2 image from left to right: 09.29.2018, 08.20.2019, 09.28.2020 (image contrast and brightness adjusted)
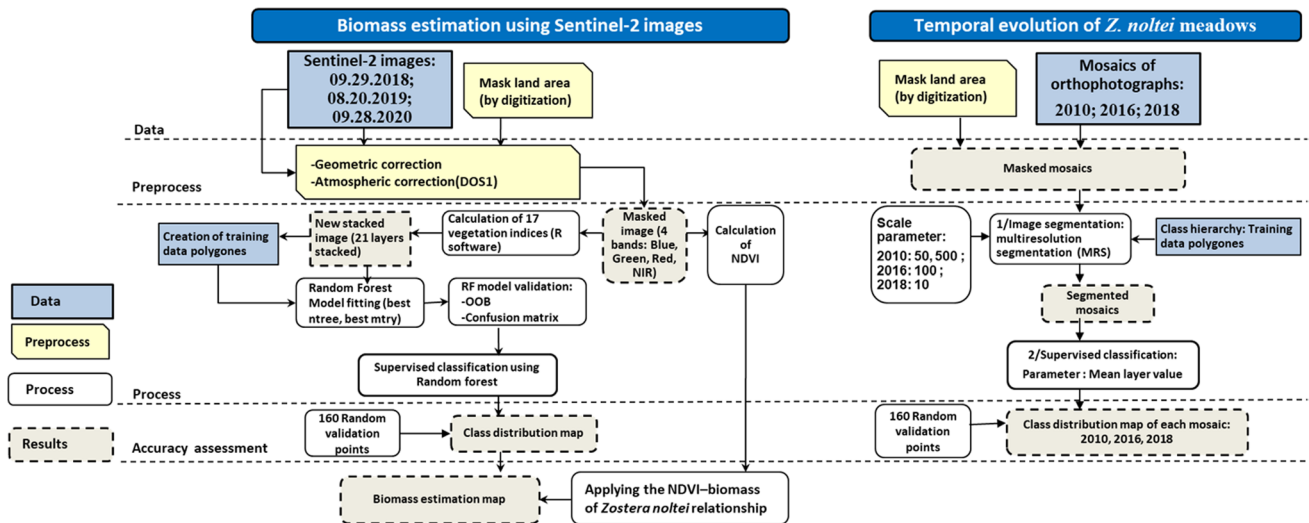
Fig. 3 Flowchart of data processing to map *Z. noltei* and algae in the Merja Zerga lagoon

118 for 08.20.2019 Sentinel-2 satellite images and 107 for 09.28.2020 Sentinel-2 satellite images (details in Table 4).

Random Forest Classification

Introduced by Breiman in 2001, random forest (RF) was proven to be more efficient than simpler classification algorithms and has generated results which are at least similar to those of other machine learning classifiers, such as Support Vector Machine and k-nearest neighbors, when applied to seagrass, coral reefs and coastal meadows Zhang 2015; Traganos and Reinartz 2018a, b; Villoslada et al. 2020).

To verify the variable importance of the random forest model, we used the Mean Decrease Gini index (MDG) to measure the impurity at each tree node split of a predictor feature, normalized by the number of trees, the highest MDG

Table 3 Sentinel-2 satellite image bands and the seventeen indices used for random forest classification

Bands and indices	Band name and full form of indices
b1	Reflectance in Blue (Band 2 of Sentinel-2 satellite)
b2	Reflectance in Green (Band 3 of Sentinel-2 satellite)
b3	Reflectance in Red (Band 4 of Sentinel-2 satellite)
b4	Reflectance in Near-Infrared (NIR) (Band 8 of Sentinel-2 satellite)
GNDVI	Green Normalized Vegetation Index (Gitelson and Merzlyak 1998)
NDVI	Normalized Vegetation Index (Rouse et al. 1974)
GVI	Green Vegetation Index (Kauth and Thomas 1976)
EVI	Enhanced Vegetation Index (Huete et al. 1994)
SAVI	Soil-Adjusted Vegetation Index (Huete and Johnson 1988)
MSAVI	Modified Soil-Adjusted Vegetation Index (Qi et al. 1994)
MSAVI2	Modified Soil-Adjusted Vegetation Index 2 (Qi et al. 1994)
NDWI	Normalized Water Index (McFeeters 1996)
RVI	Ratio Vegetation Index
NRVI	Normalized Ratio Vegetation Index (Baret and Guyot 1991)
TVI	Transformed Vegetation Index (Deering et al. 1975)
TTVI	Thiam's Transformed Vegetation Index (Thiam 1997)
SR	Simple Ratio Vegetation Index (Birth and McVey 1968)
CTVI	Corrected Transformed Vegetation Index (Perry and Lautenschlager 1984)
GEMI	Global Environmental Monitoring Index (Pinty and Verstraeta 1992)
DVI	Difference Vegetation Index (Richardson and Wiegand 1977)
EVI2	Two-band Enhanced Vegetation Index (Jiang et al. 2008)

Table 4 Total number of polygons (NP) for each land cover class and their respective average surface in m^2 (ASP) for the three Sentinel-2 satellite images 09.29.2018; 08.20.2019; 09.28.2020

Land cover classes	09.29.2018		08.20.2019		09.28.2020	
	NP	ASP	NP	ASP	NP	ASP
Algae	17	332	14	328	21	536
Shallow water	14	1326	15	3204	14	1326
Mixed algae and dwarf eelgrass	16	1143	13	730	12	697
Sand	11	528	14	2447	14	435
Mud	8	1611	13	1624	6	2540
Terrestrial plants	14	1143	21	1127	14	1143
Emergent dwarf eelgrass	12	1087	17	386	18	2296
Submerged dwarf eelgrass	8	123	11	132	8	262

value, and the purity of the variable. The higher the value of mean decrease Gini score, the higher the importance of the variable in the model (the variable here corresponds to the four raw Sentinel-2 bands and the seventeen indices). It is normal that the scale of the MDG value vary between each Sentinel-2 image.

The mtry number (number of predictors selected for splitting at each node) and ntree (number of trees) are the two essential parameters that need to be tested before tuning the random forest model (Scornet 2017). Using the best mtry number, we computed the random forest algorithm with various ntree values and recorded the out-of-bag (OOB) error rate to determine the number of trees at which the OOB error rate stabilized and reached the minimum. This allowed us to determine the ideal number of trees corresponding to a stable classifier without requiring too much computation time (in this case, different mtry and ntree best values were found for each Sentinel-2 image).

Note that when training the model, the RF classifier constructs a bootstrap sample from 2 to 3 samples of the training dataset, whereas the remaining samples, which are not included in the training subset, are used for internal error estimation known as out-of-bag (OOB) error. This and the confusion matrix (i.e. percentage of false and classified training pixels) are used to validate the random forest algorithm. Later, using the clusterR interface (in the 'raster' R package) to speed up the calculation, we used the 'predict' function to compute the RF classification prediction.

Object-Based Image Analysis

The results of an object-based image analysis (OBIA) gave us an idea of the evolution of *Z. noltei* meadow coverage in the Merja Zerga lagoon. This was investigated using the mosaics of orthophotographs registered in 2010, 2016 and 2018.

The OBIA method is carried out in two steps: image segmentation and classification, for each segment. The first step clusters pixels into image-objects by maximizing the heterogeneity between them and the homogeneity within them (Blaschke 2010). Note that the value of each segmentation parameter used is a result of test and error since there is no absolute rule to set the thresholds, so we proceeded by successive tests until we obtained a correct result in relation to the knowledge of the field (Trimble 2014). For this, we used the common image segmentation method 'multiresolution segmentation' (MRS), a non-supervised region-growing segmentation algorithm that provides useful bases for supervised classification, in particular extracting textural, spatial and spectral features (Flanders et al. 2003; Su et al. 2008). In this study, after experimenting with some object scale values, we finally used level 100 (shape 0.1, compactness 0.5) for the 2016 mosaic and level 10 (shape 0.1, compactness 0.5) for the 2018 mosaic. In terms of the 2010 mosaic, the submerged areas of *Z. noltei* were delimited by using the level 50 and the emergent ones by using level 500. For the second step in the OBIA analysis, the image-objects generated were overlaid with in-situ data so that selected objects were used to extract the features for classifying them, thus generating a habitat map (Fig. 4). The mean layer value of each of the three mosaic layers (in object features) was used as a variable to apply the OBIA classification.

The final important step before validating the classifications of Sentinel-2 image and orthophoto mosaics was to assess its accuracy using a confusion matrix (Congalton 1991; Congalton and Green 2008). This process computes an error matrix, providing information on the overall classification accuracy, the overall kappa statistics and the conditional kappa for each class (Cohen 1960; Landis and Koch 1977). A final evaluation of the quality of the 'accuracy' classification error was carried out for each image and orthophoto mosaic using Erdas software, by creating 160 equalized random points spread over the eight classes.

Seagrass Biomass Estimation Using Sentinel-2 Satellite Images

Many different vegetation indices (Vis) have previously been applied to multispectral remote sensing images to map intertidal seagrass beds (Bargain et al. 2012). NDVI seems to

Fig. 4 OBIA classification steps applied to the 2018 orthophoto mosaic (**a** MSR segmentation using level 10; **b** samples of classes assigned to objects used for classification; **c** habitat map resulting from the classification)
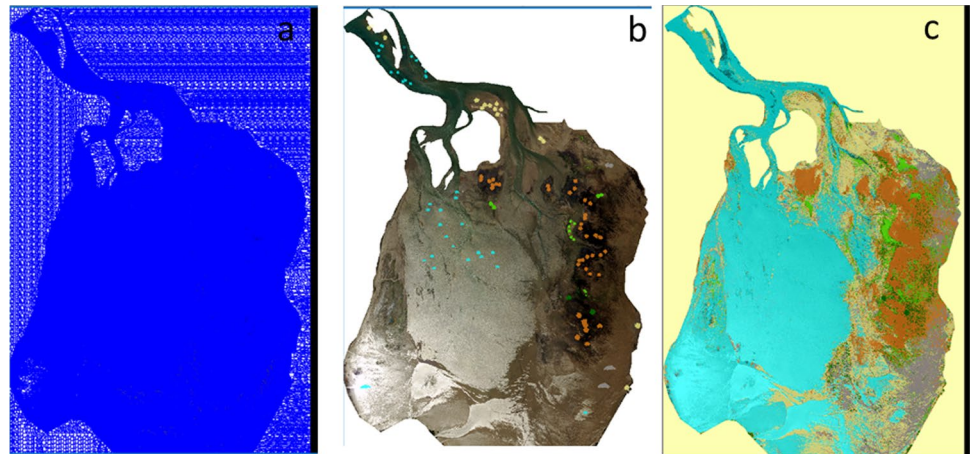
be the most appropriate vegetation index for estimating the biomass of seagrass beds, especially when using Sentinel-2 satellite images. This index enables consistent long-term studies that have been widely used and could be applied to most satellite sensors, both historical and current (Zoffoli et al. 2020).

To estimate the aboveground *Z. noltei* biomass in the Merja Zerga using remote sensing, we used the quantitative experimental NDVI – *Z. noltei* biomass relationship, whereby biomass $= 610.61$ (NDVI)$^{1.88}$ (n $= 31$, r2 $= 0.97$), as created by Barillé et al. (2010). The Sentinel-2 image classification results were used to select *Z. noltei* areas from NDVI images, which were then used to estimate the seagrass biomass. Note that the biomass estimated from pixels where *Z. noltei* beds were submerged were not considered because their NDVI results were negative and the empirical relationship was not applicable for these pixels.

Results

Random Forest Classification Results

According to the OOB values, the RF model used was robust. The index values for each Sentinel-2 image result were 2.64% for 2018, 6.72% for 2019 and 13.06% for 2020. The results for each Sentinel-2 image also showed that, of the seventeen vegetation indices used as input into the RF classification, the GNDVI and NDWI gave the highest Mean Decrease Gini score (except for the Sentinel-2 2020 image, for which EVI gave the highest MDG value) and were therefore the most important indices for discriminating between the eight classes (Fig. 5).

As a first step in this study, we estimated the coverage areas of *Z. noltei* beds based on the classification results (Fig. 4). After setting the random forest model parameters for each image, the results showed that the best parameter values were different for each image (Table 5), but all presented a good overall (OA) assessment value.

For each classified image, therefore, the total coverage area of *Z. noltei* and the specific total area for each class of *Z. noltei* beds in Merja Zerga lagoon are given (Table 6). The results show a significant progressive increase of total *Z. noltei* distribution area from 99.38 ha in 2016 to 374 ha in 2020. The classification results (Fig. 6) were then used to estimate the aboveground biomass of *Z. noltei*.

Classification Validation

To validate the RF classification results, the OOB and confusion matrix (i.e. percentage of false and classified training pixels) were estimated, based on a bootstrap sample from 2 to 3 samples of the training dataset and the remaining samples not included in the training subset. In addition to this, a second check on the classification quality was carried out as a subsequent, objective procedure to evaluate the spatialization of the classification (the extrapolation part), and not just the properties of the model. For all the data except the 2010 mosaic, we used 160 validation points distributed evenly across the eight classes to compute the confusion matrix, using ERDAS IMAGINE software. With the classification of the orthophoto 2010 mosaic, mixed beds and algae were not discernible and the downstream part of the lagoon had a higher tidal level than both the 2016 and 2018 orthophoto mosaics. As a result, and based on the segmentation results, only the objects containing *Z. noltei* were masked and then organized into three classes: submerged dwarf eelgrass, emergent dwarf eelgrass and substrate (Fig. 7). The accuracy assessment results of both types of data were therefore satisfactory; 82.50% with a minimum kappa index of 0.80 were found for the Sentinel-2 images, while an overall minimum accuracy of 78.33% with a minimum kappa index of 0.74 were found for the orthophotography mosaics (Table 7).
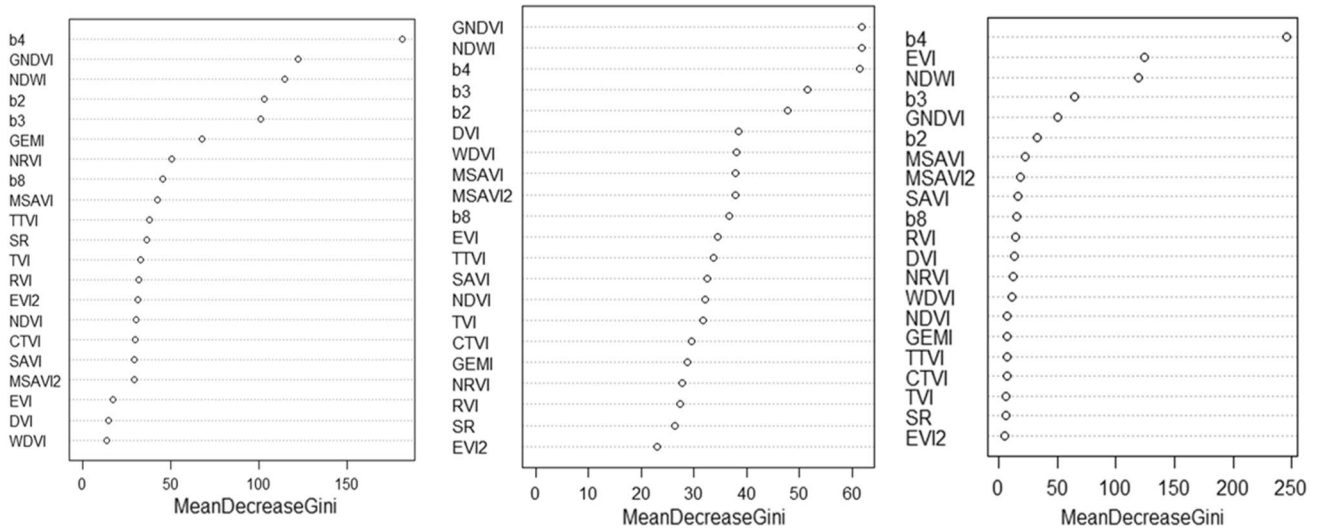
Fig. 5 Mean Decrease Gini for each Sentinel-2 image, left to right: 09.29.2018, 08.20.2019, 09.28.2020

Seagrass Biomass Estimation from Sentinel-2 Imagery

The *Z. noltei* biomass estimated using the three Sentinel-2 satellite images showed a maximum level in the eastern part of the Merja Zerga lagoon and it has reached a maximum of 231 g DW/m2 in 2020 (Fig. 8). The mean biomass of *Z. noltei* beds produced in each year was 78.49 g DW/m² for 2018, 92.59 g DW/m² for 2019 and 115.21 g DW/m² for 2020. Because the dwarf eelgrass beds coverage increased between 2018 and 2020, the estimated total biomass in 2018 would be lower, and the results indicate that the latter is only half of that estimated in 2020. However, due to the negative NDVI values for some submerged beds it was not possible to estimate their biomass, so the results are slightly underestimated.

Discussion

The results reveal that both classifications used in this study, the RF classification applied to the Sentinel-2 satellite images and the OBIA classification applied to the orthophotographs, showed good classification accuracy for

Table 5 Random forest parameters for each Sentinel-2 image

RF parameter value	09.29.2018	08.20.2019	09.28.2020
Best ntree	250	400	800
Best mtry	6	3	18
Best maxnodes	27	--	30
OA assessment %	2.64	6.72	13.06

mapping seagrass beds. The first approach achieved an average 80% overall accuracy and a kappa index higher than 0.80 while the second approach achieved 89.23% overall accuracy with a kappa index of 0.80 for 2010 mosaic, 81.25% overall accuracy with a kappa index of 0.78 for 2016 mosaic and 78.33% with a kappa index of 0.74 for 2018 mosaic. When masking *Z. noltei* beds from the other lagoon habitats for inclusion in the classification, the results were more accurate and confusion between classes very low for the 2010 mosaic. The Sentinel-2 estimate for the area occupied by *Z. noltei* beds in 2018 was less than the orthophoto estimate, the former image having been captured in September and the latter in July, demonstrating the importance of taking seasonal changes into account for this species.

Ibara et al. (2015) used the DBSCAN (Density-Based Spatial Clustering of Applications with Noise) algorithm with an IKONOS image acquired in September 2010 to identify all the wetland habitats of the Merja Zerga. They combined a supervised classification (per pixel) and an object-oriented classification (unsupervised) and estimated the area of the aquatic beds to be 256.20 ha. In contrast to our findings, this previous work took into account the substrate and algae – other components of the aquatic beds along with *Z. noltei* – rather than defining the precise boundaries of the dwarf eelgrass. In our study, the results of the 2010 orthophoto mosaic showed the extent of these beds as 143.08 ha, which constitutes the majority of the area suggested by Ibara et al. (2015).

Our results showed a slight increase in the extent of the species between 2010 and 2020, especially in the center and upstream parts of the Merja Zerga lagoon. It is also important to mention that the dwarf eelgrass beds in the eastern part of the lagoon are not completely homogeneous

Table 6 Estimated coverage areas for *Z. noltei* beds by year in the Merja Zerga lagoon, in ha (*not estimated)

Classes of *Z. noltei* beds	Mosaic 2010	Mosaic 2016	Mosaic 2018	09.29.2018	08.20.2019	09.28.2020
submerged *Z. noltei*	0.93	25.97	17.05	35.17	101.29	15
emergent *Z. noltei*	142.15	43.17	289.79	37.55	115.10	289
mixed beds: *Z. noltei*/Algae	*	30.25	103.94	125.56	104.37	70
Total area in Ha	143.084	99.38	317.74	198.28	320.75	374

due to the spread of opportunistic seaweed species that also occupy this habitat (Fig. 9). This is due to pressures generated by the people who live in the vicinity of the Merja Zerga lagoon, in particular the intensification of agriculture since the 1970s, with irrigation and the use of fertilizers and chemicals, especially pesticides, which despite the significant contribution they have made to increasing agricultural production are partly responsible for the diffuse pollution and deterioration of water quality for the lagoon ecosystem. Several studies have shown the presence of high levels of pesticides and sediments in the water (Mehdaoui et al. 2001; Ayadi et al. 2013; Maanan et al. 2013). The discharge of various pollutant substances of terrestrial origin (detergents,

pesticides, hydrocarbons, etc.) into continental waters lowers the vitality of individual species and can induce the propagation of green algae, which is responsible for total suffocation of the meadows due to the abundance of nutrients (Pergent-Martini 2000; Burkholder et al. 2007).

Dehouck et al. (2012), experienced difficulty in differentiating dwarf eelgrass from green algae in their interpretation of multispectral optical images, and could only discriminate the algae by using fine spectral bands in a multitemporal database. High-resolution sensors like SPOT-7 (1.5 m pixels) and Pléiades 1 A and Pléiades 1B satellites, which deliver 0.5 m imagery products with a 20 km swath, or WorldView with almost 0.3–0.4 m pixels, can counteract
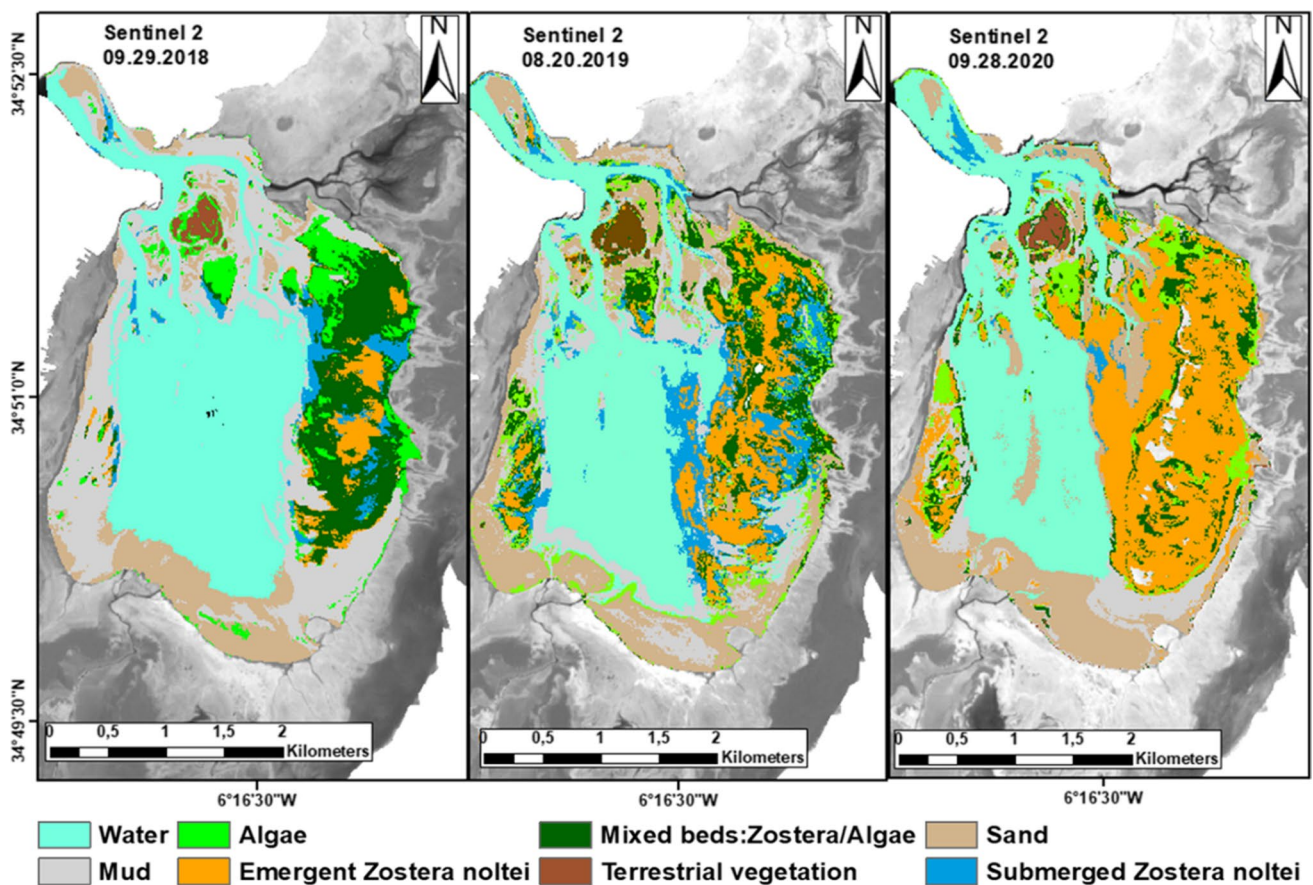
Fig. 6 Distribution of the eight classes of habitat in the Merja Zerga lagoon based on results of random forest classification for the Sentinel-2 images, left to right: 09.29.2018, 08.20.2019, 09.28.2020
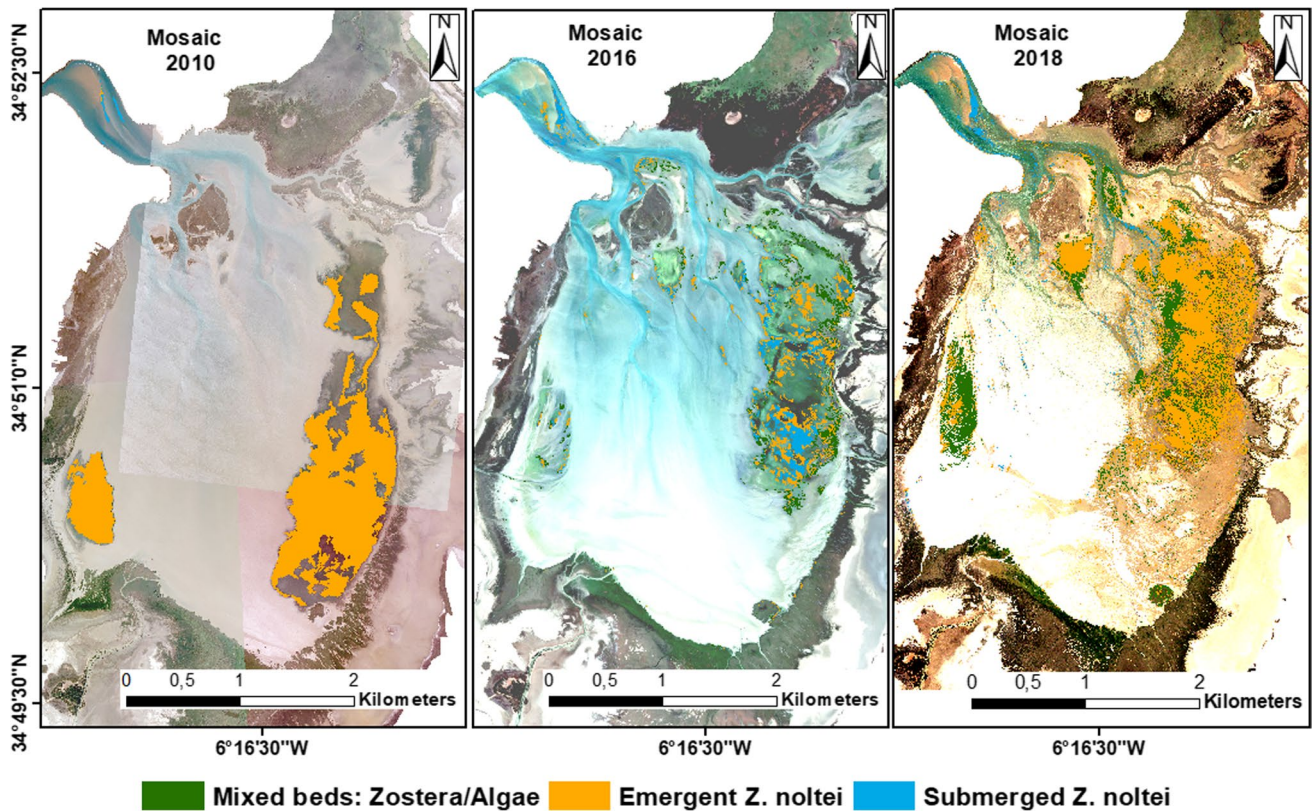
Fig. 7 Distribution of dwarf eelgrass *Z. noltei* beds in the Merja Zerga lagoon based on eCognition classification results from 2010, 2016 and 2018 mosaics

the limitations of Sentinel-2 (10 m pixels) for detecting smaller patches of seagrass and limiting the confusion of mixed pixels, but this requires funding.

Sentinel-2 data have been widely used to map different habitats and several studies have demonstrated their reliability in mapping and monitoring changes in marine biocenoses such as coral (Hedley et al. 2012), mangrove (Pham et al. 2019b, 2020) and seagrass beds Topouzelis et al. 2016; Traganos and Reinartz 2018b; Ha et al. 2020, 2021; Wicaksono et al. 2021; Nur et al. 2021; Ivajnšič et al. 2022; Hartoni et al. 2022). Many authors have used vegetation indices as the input for RF classification to map plant communities in terrestrial wetlands (Fletcher 2016) and coastal wetlands (Zoffoli et al. 2020; Martínez Prentice et al. 2021; Benmokhtar et al. 2021), and compared to many machine learning algorithms and support vector machine techniques,

the RF algorithm has produced promising results in terms of classifying seagrass (Zhang et al. 2013; Traganos and Reinartz 2018b; Ha et al. 2020). For example, to monitor the dynamics of the *Posidonia oceanica* (L.) Delile meadows and *Cymodocea nodosa* (Ucria) Ascherson meadows in the Eastern Mediterranean, Traganos and Reinartz (2018a) used the random forest algorithm and support vector machines for the RapidEye time series, after adjusting the atmospheric and analytical water column. Object-based image analysis has also been also widely used for mapping marine habitats such as corals (Roelfsema et al. 2013) and seagrass beds (Hobley et al. 2021). This process has the potential to improve classification performance (Poursanidis et al. 2018), as demonstrated with seagrass (Roelfsema et al. 2014; Duffy et al. 2018).

Table 7 Evaluation of accuracy assessment of the 2010, 2016 and 2018 orthophotography mosaics and the 2018, 2019 and 2020 Sentinel-2 images classified with RF algorithm

| Image date	2010	2016	2018	09.29.2018	08.20.2019	09.28.2020
Overall accuracy	94.44%	81.25%	78.33%	88.13%	82.50%	88.75%
Kappa index	0.92	0.78	0.74	0.86	0.80	0.87
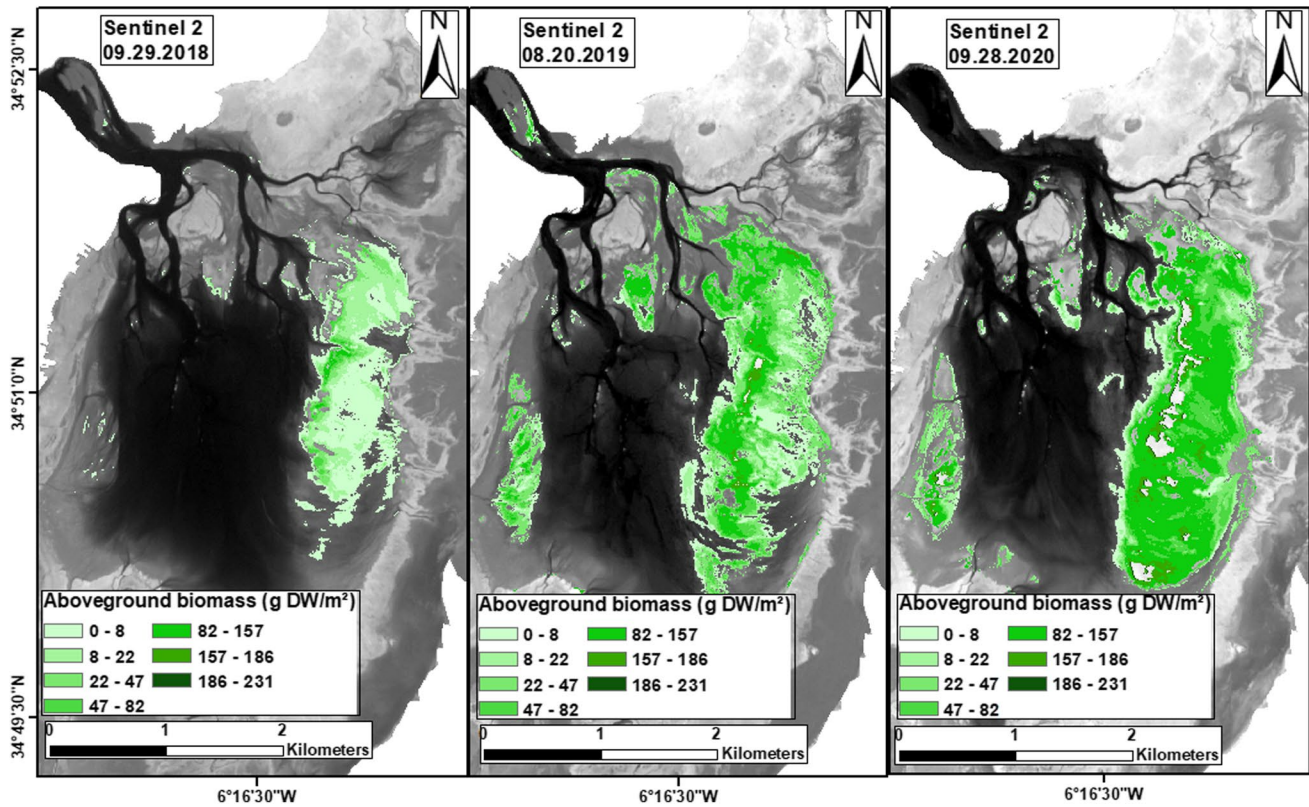
Fig. 8 Aboveground biomass estimated from the NDVI-Sentinel-2 image: 09.29.2018, 08.20.2019, 09.28.2020

Over the years, the availability of satellite imagery and aerial photos has often complemented traditional in-situ field surveys Traganos and Reinartz 2018a, b; Roelfsema et al. 2014; Topouzelis et al. 2018). The first results of our work were typically maps of the presence or absence of seagrass and its spatial extent. Quantitative information on density and biomass cannot be achieved using the classification results alone (Price et al. 2022). The empirical relationship between field data and vegetation indices revealed by high hyperspectral or multispectral satellite imagery can provide biomass and density maps (Barillé et al. 2010; Bargain et al. 2013; Roelfsema et al. 2014; Benmokhtar et al. 2021), and the biomass of the *Z. noltei* beds in Merja Zerga lagoon was estimated using the quantitative experimental NDVI – *Z*.
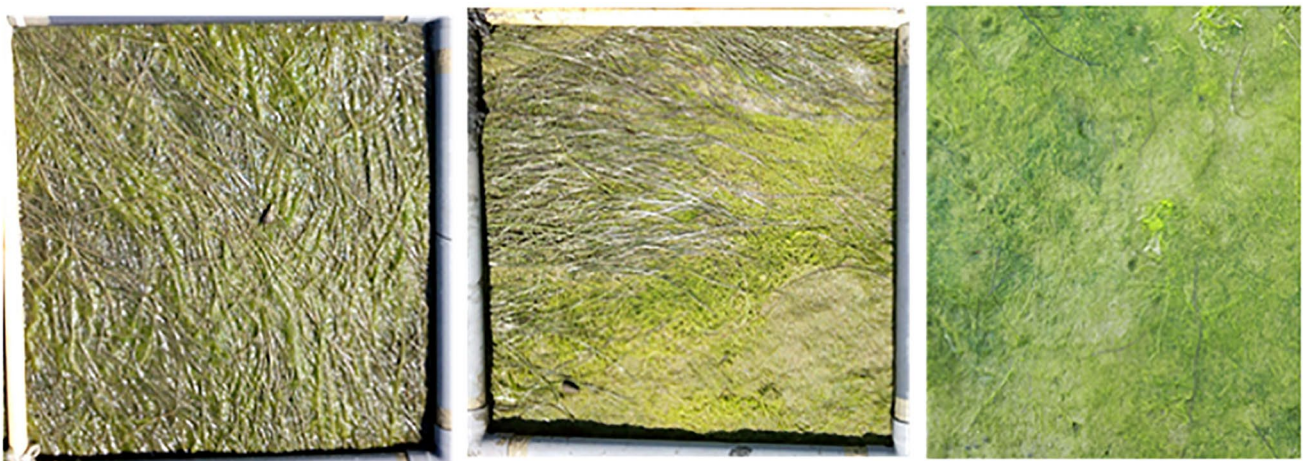
Fig. 9 Field photography of three densities of *Z. noltei* beds showing the presence of opportunistic green algae

noltei biomass relationship created by Barillé et al. (2010), whereby biomass = 610.61 (NDVI)^1.88 (n = 31, r2 = 0.97). The NDVI–biomass quantitative model applied to satellite image data is useful as a non-destructive method for estimating seagrass and microphytobenthos biomass (Zoffoli et al. 2020, 2021), and when we applied this method to the Sentinel-2 data, we found that *Z. noltei* biomass reached a maximum of 231 g DW/m² in 2020. However, this result may be slightly lower than the actual biomass; when Sentinel-2 images were processed to NDVI, the submerged *Z. noltei* bed classification contained some negative NDVI values that could not be used for estimating the biomass, so the total figure for *Z. noltei* biomass did not include these pixels.

In this study, the highest level of dwarf eelgrass biomass was observed in 2020, and coincided with a suspension of shellfish harvesting and tourism due to the national lockdown in response to the Covid-19 pandemic. However, the causality remains to be established. The identification of anthropogenic and environmental factors driving the temporal variability of *Z. noltei* in the Merja Zerga lagoon is not within the scope of the present study and will be investigated in future works.

The approach of our study is replicable, inexpensive, and easily transferable to biodiversity conservation interests for long-term use, as it employs the open-source Sentinel-2 data processed with geoinformatics freeware. Marine spatial managers and other stakeholders can therefore employ the maps to analyze links between seagrass coverage and the ecosystem services it provides, such as carbon sequestration and biodiversity.

Conclusion

Z. noltei beds can be mapped successfully using Sentinel-2 imagery and orthophoto mosaics with high spatial resolution. By combining the 10 m spatial resolution of Sentinel-2 satellite images with field data, the extent of dwarf eelgrass beds can be monitored and their aboveground biomass accurately assessed, and the random forest algorithm can be used to classify these types of data and differentiate between dwarf eelgrass beds and other types of habitats in the intertidal zone, in particular macroalgae. Unlike orthophoto mosaics, the Sentinel-2 satellite image data is an open-source resource available via the ESA sci-hub and EU Copernicus portals, and is therefore an excellent solution for mapping *Z. noltei* beds at no cost. The present study is the first to monitor interannual changes in *Z. noltei* beds in the Merja Zerga lagoon using different types of remote sensing data. In addition, potential terrestrial vegetation should be removed from the satellite image and orthophoto mosaics before running the classification algorithm which will minimize confusion with these habitats. It is also important to

consider acquiring data imagery with the lowest possible tide level and high spatial resolution, which some previous authors have overlooked when mapping seagrass beds in this wetland and have consequently obtained results that underestimate their extent. The technique used here to calculate biomass is a practical one that does not harm this specie' beds. The same approach as the one used in this study can be used in future works that involve monitoring *Z. noltei* beds and estimating their biomass with similar results, and better results can be achieved with higher resolution imagery data which are not free of charge.

Author Contributions All authors contributed to the study conception and methodology: the conceptualization was performed by Benmokhtar Salma, Bazairi Hocein, Robin Marc and Maanan Mohamed; the methodology was realized by Benmokhtar Salma, Bazairi Hocein, Robin Marc, Badaoui Bouabid and Boutoumit Soilam; the writing—review and editing was carried out by Benmokhtar Salma, Bazairi Hocein, Robin Marc, Maanan Mohamed and Badaoui Bouabid. All authors have read and agreed to the published version of the manuscript.

Data Availability The data that support the findings of this study would be available upon request from the authors.

Declarations

Competing Interests The authors have no relevant financial or non-financial interests to disclose.

References

Alaoui AM, Choura M, Maanan M, Zourarah B, Robin M, Conceição MF, Andrade C, Khalid M, Carruesco C (2010) Metal fluxes to the sediments of the Moulay Bousselham lagoon, Morocco. Environmental Earth Sciences 61:275–286. https://doi.org/10.1007/s12665-009-0341-9

Appleby PG, Birks HH, Flower RJ, Rose N, Peglar SM, Ramdani M, Kraïem MM, Fathi AA (2001) Radiometrically determined dates and sedimentation rates for recent sediments in nine north african wetland lakes (the CASSARINA Project). Aquatic Ecology 35:347–367. https://doi.org/10.1023/A:1011938522939

Ayadi H, Le Marjorie M, Le Ph G, Mandart E, Fabre J, Bouaziz A, Bord J-P (2013) SimPhy: a simulation game to lessen the impact of phytosanitaries on health and the environment–- the case of Merja Zerga in Morocco. Environmental Science and Pollution Research 21:4950–4963. https://doi.org/10.1007/s11356-013-2244-2

Baret F, Guyot G (1991) Potentials and limits of vegetation indices for LAI and APAR assessment. Remote Sensing of Environment 35:161–173

Bargain A, Robin M, le Men E, Huete A, Barillé L (2012) Spectral response of the seagrass Zostera noltii with different sediment backgrounds. Aquatic Botany 98:45–56. https://doi.org/10.1016/j.aquabot.2011.12.009

Bargain A, Robin M, Meleder V, Rosa P, Le Menn E, Harin N, Barille L (2013) Seasonal spectral variation of Zostera noltii and its influence on pigment-based Vegetation Indices. Journal of Experimental Marine Biology and Ecology 446:86–94. https://doi.org/10.1016/j.jembe.2013.04.012

Barillé L, Robin M, Harin N, Bargain A, Launeau P (2010) Increase in seagrass distribution at Bourgneuf Bay (France) detected by spatial remote sensing. Aquatic Botany 92:185–194. https://doi.org/10.1016/j.aquabot.2009.11.006

Bazaïri H, Bayed A, Glémarec M, Hily C (2003) Spatial organization of macrozoobenthic communities in response to environmental factors in a coastal lagoon of the NW African coast (Merja Zerga, Morocco). Oceanologica Acta 26:457–471. https://doi.org/10.1016/S0399-1784(03)00041-0

Benmokhtar S, Robin M, Maanan M, Bazairi H (2021) Mapping and quantification of the dwarf eelgrass Zostera noltei using a Random Forest Algorithm on a SPOT 7 Satellite Image. ISPRS International Journal of Geo-Information 10:313. https://doi.org/10.3390/ijgi10050313

Birth GS, McVey G (1968) Measuring the color of growing turf with a reflectance spectroradiometer. Agronomy Journal 60:640–643

Blaschke T (2010) Object based image analysis for remote sensing. ISPRS J Photogramm ISPRS J Photogramm Remote Sens 65:2–16. https://doi.org/10.1016/j.isprsjprs.2009.06.004

Bououarour O, El Kamcha R, Boutoumit S, Pouzet P, Maanan M, Bazairi H (2021) Effects of the Zostera noltei meadows on benthic macrofauna in North Atlantic coastal ecosystems of Morocco: spatial and seasonal patterns. Biologia 76:1–13. https://doi.org/10.1007/s11756-021-00718-9

Boutahar L, Maanan M, Bououarour O, Richir J, Pouzet P, Gobert S, Maanan M, Zourarah B, Benhoussa A, Bazairi H (2019) Biomonitoring environmental status in semi-enclosed coastal ecosystems using Zostera noltei meadows. Ecological Indicators 104:776–793. https://doi.org/10.1016/j.ecolind.2019.04.039

Breiman L (2001) Random forests. Machine Learning 45:5–32

Burkholder JM, Tomasko DA, Touchette BW (2007) Seagrasses and eutrophication. Journal of Experimental Marine Biology and Ecology 350:46–72. https://doi.org/10.1016/j.jembe.2007.06.024

Cabaço S, Santos R, Sprung M (2011) Population dynamics and production of the seagrass Zostera noltii in colonizing versus established meadows. Marine Ecology 33:280–289. https://doi.org/10.1111/j.1439-0485.2011.00494.x

Chust G, Borja Á, Caballero A, Irigoien X, Sáenz J, Moncho R, Marcos M, Liria P, Hidalgo J, Valle M, Valencia V (2011) Climate change impacts on coastal and pelagic environments in the southeastern Bay of Biscay. Climate Research 48:307–332. https://doi.org/10.3354/cr00914

Cohen J (1960) A coefficient of agreement for nominal scales. Educational and Psychological Measurement 20:37–46. https://doi.org/10.1177/001316446002000104

Congalton RG (1991) A review of assessing the accuracy of classifications of remotely sensed data. Remote Sensing of Environment 37:35–46. https://doi.org/10.1016/0034-4257(91)90048-B

Congalton RG, Green K (2008) Assessing the accuracy of remotely sensed data: Principles and practices, Second Edition (2nd edn). CRC Press., Lewis Publishers, Boca Raton, 137p. https://doi.org/10.1201/9781420055139

Dalloyau S (2020) Qualité Ecologique des Herbiers Intertidaux à Zostère Naine Zostera Noltei dans les Sites Fonctionnels des Réserves Naturelles Nationales Gérées par la LPO (Pertuis Charentais). https://www.researchgate.net/publication/349345847_Qualite_ecologique_des_herbiers_intertidaux_a_Zostere_naine_Zostera_noltei_dans_les_sites_fonctionnels_des_Reserves_Naturelles_Nationales_gerees_par_la_LPO_Pertuis_Charentais. Accessed 04 June 2022

Deering DW, Rouse JW, Haas RH, Schell JA (1975) Measuring "Forage Production" of grazing units from landsat MSS data, proceedings of the 10th International Symposium on Remote Sensing of Environment, 2, 1169–1178

Dehouck A, Lafon V, Lubac B, Kervella S, Bru D, Schmeltz M, Roubache A (2012) Hyperspectral field database in support to coastal wetland mapping. In: Proceedings of the 2012 IEEE International Geoscience and Remote Sensing Symposium. Munich, Germany, pp 2649–2652

Diekmann OE, Gouveia L, Perez JA, Gil-Rodriguez C, Serrão EA (2010) The possible origin of Zostera noltii in the Canary Islands and guidelines for restoration. Marine Biology 157:2109–2115. https://doi.org/10.1007/s00227-010-1467-8

Duffy JP, Pratt L, Anderson K, Land PE, Shutler JD (2018) Spatial assessment of intertidal seagrass meadows using optical imaging systems and a lightweight drone. Estuarine, Coastal and Shelf Science 200:169–180. https://doi.org/10.1016/j.ecss.2017.11.001

Ferguson RL, Wood LL, Graham DB (1993) Monitoring spatial change in seagrass habitat with aerial photography. Photogrammetric Engineering & Remote Sensing 59(6):1033–1038

Flanders D, Hall-Beyer M, Pereverzoff J (2003) Preliminary evaluation of eCognition object-based software for cut block delineation and feature extraction. Canadian Journal of Remote Sensing 29:441–452. https://doi.org/10.5589/m03-006

Fletcher RS (2016) Using vegetation indices as Input into Random forest for soybean and weed classification. American Journal of Plant Sciences 07:2186–2198. https://doi.org/10.4236/ajps.2016.715193

Flower RJ, Thompson JR (2008) An overview of integrated hydro-ecological studies in the MELMARINA Project: monitoring and modelling coastal lagoons—making management tools for aquatic resources in North Africa. Hydrobiologia (Incorporating JAQU) 622:3–14. https://doi.org/10.1007/s10750-008-9674-8

Gitelson AA, Merzlyak MN (1998) Remote sensing of chlorophyll concentration in higher plant leaves. Advances in Space Research 22:689–692. https://doi.org/10.1016/S0273-1177(97)01133-2

Green ER, Short FT (2003) World Atlas of Seagrasses. UNEP World Conservation Monitoring Center. University of California Press, Berkeley, p 332

Ha NT, Manley-Harris M, Pham TD, Hawes I (2020) A comparative assessment of ensemble-based machine learning and maximum likelihood methods for mapping seagrass using sentinel-2 imagery in Tauranga Harbor, New Zealand. Remote Sensing 12:355. https://doi.org/10.3390/rs12030355

Ha NT, Manley-Harris M, Pham TD, Hawes I (2021) The use of radar and optical satellite imagery combined with advanced machine learning and metaheuristic optimization techniques to detect and quantify above ground biomass of intertidal seagrass in a New Zealand estuary. International Journal of Remote Sensing 42:4712–4738. https://doi.org/10.1080/01431161.2021.1899335

Hammada S (2007) Etudes sur la Végétation des zones Humides du Maroc: Catalogue et analyse de la Biodiversité Floristique et Identification des Principaux Groupements Végétaux. Université Mohammed V-Agdal, Faculté des Sciences Rabat, Rabat, Morocco

Hartoni, Siregar VP, Wouthuyzen S, Agus SB (2022) Object based classification of benthic habitat using Sentinel-2 imagery by applying with support vector machine and random forest algorithms in shallow waters of Kepulauan Seribu, Indonesia. Biodiversitas 23:514–520. https://doi.org/10.13057/biodiv/d230155

Hedley JD, Roelfsema CM, Phinn SR, Mumby PJ (2012) Environmental and sensor limitations in optical remote sensing of Coral Reefs: implications for monitoring and sensor design. Remote Sensing 4:271–302. https://doi.org/10.3390/rs4010271

Hobley B, Arosio R, French G, Bremner J, Dolphin T, Mackiewicz M (2021) Semi-supervised segmentation for coastal monitoring seagrass using RPA imagery. Remote Sensing 13:1741. https://doi.org/10.3390/RS13091741

Hossain MS, Hashim M (2019) Potential of Earth Observation (EO) technologies for seagrass ecosystem service assessments. International Journal of Applied Earth Observation and Geoinformation 77:15–29. https://doi.org/10.1016/j.jag.2018.12.009

Hossain MS, Bujang JS, Zakaria MH, Hashim M (2015) Application of landsat images to seagrass areal cover change analysis for Lawas, Terengganu and Kelantan of Malaysia. Continental Shelf Research 110:124–148. https://doi.org/10.1016/j.csr.2015.10.009

Huete A, Jackson R (1988) Soil and atmosphere influences on the spectra of partial canopies. Remote Sensing of Environment 25:89–105. https://doi.org/10.1016/0034-4257(88)90043-0

Huete A, Justice C, Liu H (1994) Development of vegetation and soil indices for MODIS-EOS. Remote Sensing of Environment 49:224–234. https://doi.org/10.1016/0034-4257(94)90018-3

Ibara BO, Dakki M, Hakdaoui M, El Hamoumi R (2015) Contribution of hybrid classification on IKONOS satellite imagery in mapping of wetland's habitats: Merja Zerga (Morocco). International Journal of Innovation and Applied Studies ISSN 12:851–863

Ivajnšič D, Orlando-Bonaca M, Donša D, Grujić VJ, Trkov D, Mavrič B, Lipej L (2022) Evaluating seagrass meadow dynamics by integrating field-based and remote sensing techniques. Plants 11:1196. https://doi.org/10.3390/plants11091196

Jiang Z, Huete AR, Didan K, Miura T (2008) Development of a two-band enhanced vegetation index without a blue band. Remote Sensing of Environment 112:3833–3845. https://doi.org/10.1016/j.rse.2008.06.006

Kauth RJ, Thomas GS (1976) Tasselled Cap - A graphic description of the spectral-temporal development of agricultural crops as seen by Landsat. LARS Symposia. Proceedings of the Symposium on Machine Processing of the Remotely Sensed Data, Purdue University, West -Lafayette, 159:41–51. https://www.google.com/url?sa=t&rct=j&q=&esrc=s&source=web&cd=&cad=rja&uact=8&ved=2ahUKEwjlgsLE9-b4AhUI4RoKHbu6CK0QFnoECAYYAQ&url=https%3A%2F%2Fdocs.lib.purdue.edu%2Flars_symp%2F159%2F&usg=AOvVaw27isUsQ0bQruVF1FAPLITm

Kendrick GA, Aylward MJ, Hegge BJ, Cambridge ML, Hillman K, Wyllie A, Lord DA (2002) Changes in seagrass coverage in Cockburn Sound, Western Australia between 1967 and 1999. Aquatic Botany 73:75–87

Kirkman H (1996) Baseline and monitoring methods for seagrass meadows. Journal of Environmental Management 47:191–201

Kovacs E, Roelfsema C, Lyons M, Zhao S, Phinn S (2018) Seagrass habitat mapping: how do landsat 8 OLI, Sentinel-2, ZY-3A, and Worldview-3 perform? Remote Sensing Letters 9:686–695. https://doi.org/10.1080/2150704X.2018.1468101

Kraiem M, Ben Hamza C, Ramdani M, Fathi A, Abdelzaher H, Flower R (2001) Some observations on the age and growth of thin-lipped grey mullet, Liza ramada Risso, 1826 (Pisces, Mugilidae) in three north african wetland lakes: Merja Zerga (Morocco), Garâat Ichkeul (Tunisia) and Edku Lake (Egypt). Aquatic Ecology 35:335–345. https://doi.org/10.1023/a:1011900631096

Labbardi H, Ettahiri O, Lazar S, Massik Z, El Antri S (2005) Étude de la variation spatio-temporelle des paramètres physico-chimiques caractérisant la qualité des eaux d'une lagune côtière et ses zonations écologiques: Cas de Moulay Bousselham, Maroc. Comptes Rendus Geoscience 337:505–514. https://doi.org/10.1016/j.crte.2005.01.009

Landis R, Koch GG (1977) The measurement of observer agreement for categorical data. Biometrics 33:159–174. https://doi.org/10.2307/2529310

Lyons MB, Phinn SR, Roelfsema CM (2011) Integrating Quickbird multi-spectral satellite and field data: mapping bathymetry, sea-grass cover, seagrass species and change in Moreton Bay, Australia in 2004 and 2007. Remote Sensing 3:42–64. https://doi.org/10.3390/rs3010042

Lyons MB, Roelfsema CM, Phinn SR (2013) Towards understanding temporal and spatial dynamics of seagrass landscapes using time-series remote sensing. Estuarine, Coastal and Shelf Science 120:42–53. https://doi.org/10.1016/J.ECSS.2013.01.015

Maanan M, Landesman C, Maanan M, Zourarah B, Fattal P, Sahabi M (2013) Evaluation of the anthropogenic influx of metal and metalloid contaminants into the Moulay Bousselham lagoon, Morocco, using chemometric methods coupled to geographical information systems. Environmental Science and Pollution Research 20:4729–4741. https://doi.org/10.1007/s11356-012-1399-6

Martínez Prentice R, Villoslada Peciña M, Ward RD, Bergamo TF, Joyce CB, Sepp K (2021) Machine learning classification and accuracy assessment from high-resolution images of coastal wetlands. Remote Sensing 13:3669. https://doi.org/10.3390/rs13183669

McFeeters SK (1996) The use of the normalized difference water index (ndwi) in the delineation of open water features. International Journal of Remote Sensing 17:1425–1432. https://doi.org/10.1080/01431169608948714

Mehdaoui O, Venant A, Fekhaoui M (2001) Contamination par les pesticides organochlorés et les nitrates de la lagune de Moulay Bousselham, Maroc. Cahiers d'études et de recherches francophones/Santé 10(6):381–388. https://doi.org/10.1109/IGARSS.2012.6350384

Misbari S, Hashim M (2016) Change detection of submerged seagrass biomass in shallow coastal water. Remote Sensing 8(3):200. https://doi.org/10.3390/rs8030200

Nur S, Nurdjaman S, Dika B, Cahya PP, Al-ghifari KHD (2021) Integrating sentinel-2 spectral-imagery and field data of seagrass coverage with species identification in the coastal of Riau Islands, Indonesia. Borneo Journal of Marine Science and Aquaculture 05(02):78–82. https://doi.org/10.51200/bjomsa.v5i2.2710

Orth RJ, Carruthers TJB, Dennison WC, Duarte CM, Fourqurean JW, Heck KL, Hughes AR, Kendrick GA, Kenworthy WJ, Olyarnik S, Short FT, Waycott M, Williams SL (2006) A global crisis for seagrass ecosystems. BioScience 56:987–996. https://doi.org/10.1641/0006-3568(2006)56[987:AGCFSE]2.0.CO;2

Pergent-Martini C (2000) Protection des habitats d'herbiers de phanérogames marines de Méditerranée – Les études d'impacts en milieu marin. CAR/ASP Tunis et EqEL publ.: 1–52 + Annexes

Perry CJr, Lautenschlager LF (1984) Functional equivalence of spectral vegetation indices. Remote Sensing of Environment 14:169–182. https://doi.org/10.1016/0034-4257(84)90013-0

Pham TD, Xia J, Ha NT, Bui DT, Le NN, Tekeuchi W (2019a) A review of Remote sensing approaches for monitoring Blue Carbon Ecosystems: Mangroves, Seagrasses and Salt Marshes during 2010–2018. Sensors 19:1933. https://doi.org/10.3390/s19081933

Pham TD, Yokoya N, Bui DT, Yoshino K, Friess DA (2019b) Remote sensing approaches for monitoring mangrove species, structure, and biomass: Opportunities and challenges. Remote Sensing 11:230. https://doi.org/10.3390/rs11030230

Pham TD, Le NN, Ha NT, Nguyen LV, Xia J, Yokoya N, To TT, Trinh HX, Kieu LQ, Takeuchi W (2020) Estimating mangrove above-ground biomass using extreme gradient boosting decision trees algorithm with fused Sentinel-2 and ALOS-2 PALSAR-2 data in

Can Gio Biosphere Reserve, Vietnam. Remote Sensing 12:777. https://doi.org/10.3390/rs12050777

Phinn S, Roelfsema C, Dekker A, Brando V, Anstee J (2008) Mapping Seagrass Species, cover and biomass in shallow Waters: an Assessment of Satellite Multi-Spectral and Airborne Hyper-Spectral Imaging Systems in Moreton Bay (Australia). Remote Sensing of Environment 112:3413–3425. https://doi.org/10.1016/j.rse.2007.09.017

Pinty B, Verstraete MM (1992) GEMI: a non-linear index to monitor global vegetation from satellites. Plant Ecology 101:15–20

Polte P, Schanz A, Asmus H (2005) The contribution of seagrass beds (Zostera noltii) to the function of tidal flats as a juvenile habitat for dominant, mobile epibenthos in the Wadden Sea. Marine Biology 147:813–822. https://doi.org/10.1007/s00227-005-1583-z

Poursanidis D, Topouzelis K, Chrysoulakis N (2018) Mapping coastal marine habitats and delineating the deep limits of the Neptune's seagrass meadows using VHR earth observation data. International Journal of Remote Sensing 39(23):8670–8687. https://doi.org/10.1080/01431161.2018.1490974

Price DM, Felgate SL, Huvenne VAI, Strong J, Carpenter S, Barry C, Lichtschlag A, Sanders R, Carrias A, Young A, Andrade V, Cobb E, Le Bas T, Brittain H, Evans C (2022) Quantifying the Intra-Habitat Variation of Seagrass Beds with Unoccupied Aerial Vehicles (UAVs). 14:480. https://doi.org/10.3390/rs14030480

Prieto-Amparan JA, Villarreal-Guerrero F, Martinez-Salvador M, Manjarrez-Domínguez C, Santellano-Estrada E, Pinedo-Alvarez A (2018) Atmospheric and radiometric correction algorithms for the multitemporal assessment of grasslands productivity. Remote Sensing 10:219. https://doi.org/10.3390/rs10020219

Pu R, Bell S (2013) A protocol for improving mapping and assessing of seagrass abundance along the West Central Coast of Florida using landsat TM and EO-1 ALI / Hyperion images. ISPRS Journal of Photogrammetry and Remote Sensing 83:116–129. https://doi.org/10.1016/j.isprsjprs.2013.06.008

Qi J, Chehbouni A, Huete AR, Kerr YH, Sorooshian S (1994) A modified soil adjusted vegetation index. Remote Sensing of Environment 48:119–126. https://doi.org/10.1016/0034-4257(94)90134-1

Rende SF, Bosman A, di Mento R, Bruno F, Lagudi A, Irving AD, Dattola L, di Giambattista L, Lanera P, Proietti R, Parlagreco L, Stroobant M, Cellini E (2020) Ultra-high-resolution mapping of Posidonia oceanica(L.) Delile Meadows through acoustic, optical data and object-based image classification. J Mar Sci Eng 8:647. https://doi.org/10.3390/jmse8090647

Richardson AJ, Wiegand CL (1977) Distinguishing vegetation from soil background information. Photogrammetric Engineering and Remote Sensing 43:1541–1552

Roelfsema CM, Phinn SR, Udy NS, Maxwell PS (2009) An integrated field and remote sensing approach for mapping Seagrass Cover, Moreton Bay, Australia. Journal of Spatial Science 54:45–62. https://doi.org/10.1080/14498596.2009.9635166

Roelfsema C, Phinn S, Jupiter S, Comley J, Albert S (2013) Mapping coral reefs at reef to reef-system scales, 10s – 1000s km, using object-based image analysis. International Journal of Remote Sensing 34:6367–6388. https://doi.org/10.1080/01431161.2013.800660

Roelfsema CM, Lyons M, Kovacs EM, Maxwell P, Saunders MI, Samper-Villarreal J, Phinn SR (2014) Multi-temporal mapping of seagrass cover, species and biomass: a semi-automated object based image analysis approach. Remote Sensing of Environment 150:172–187. https://doi.org/10.1016/j.rse.2014.05.001

Rouse J, Haas R, Schell J, Deering D (1974) Monitoring vegetation systems in the Great Plains with ERTS. In: Fraden SC, Marcanti EP, Becker M.A, eds. NASA. Goddard Space Flight Center 3d ERTS-1 Symposium, Vol.1. NASA, Texas, pp 309–317

Scornet E (2017) Tuning parameters in random forests. ESAIM: Proceedings and Surveys 60:144–162. https://doi.org/10.1051/proc/201760144

Serrano O, Kelleway JJ, Lovelock C, Lavery PS (2019) Conservation of blue carbon ecosystems for climate change mitigation and adaptation. Coastal Wetlands: An Integrated Ecosystem Approach, 965–996. https://doi.org/10.1016/B978-0-444-63893-9.00028-9

Short FT, Coles RG (2001) Global seagrass research method. Elsevier Science, Amsterdam, 33, 473

Short FT, Neckles HA (1999) The effects of global climate change on seagrasses. Aquatic Botany 63:169–196. https://doi.org/10.1016/s0304-3770(98)00117-x

Stankovic M, Ambo-Rappe R, Carly F, Dangan-Galon F, Fortes MD, Hossain MS, Kiswara W, Van Luong C, Minh-Thu P, Mishra AK et al (2021) Quantification of blue carbon in seagrass ecosystems of Southeast Asia and their potential for climate change mitigation. Science of the Total Environment 783:146858. https://doi.org/10.1016/j.scitotenv.2021.146858

Su W, Li J, Chen Y, Liu Z, Zhang J, Low TM, Suppiah I, Hashim SAM (2008) Textural and local spatial statistics for the object-oriented classification of urban areas using high resolution imagery. International Journal of Remote Sensing 29:3105–3117. https://doi.org/10.1080/01431160701469016

Tamondong A, Cruz C, Quides RR, Garcia M, Cruz JA, Guihawan J, Blanco A (2018) Remote sensing-based estimation of seagrass percent cover and LAI for above ground carbon sequestration mapping. In: Remote Sensing of the Open and Coastal Ocean and Inland Waters. SPIE. Asia-Pacific Remote Sensing. Honolulu, Hawaii, United States. 10778, 1077803. https://doi.org/10.1117/12.2324695

Thiam AK (1997) Geographic information systems and remote sensing methods for assessing and monitoring land degradation in the Sahel: The Case of Southern Mauritania. PhD Thesis. Clark University, Worcester Massachusetts

Thompson JR, Flower RJ, Ramdani M, Ayache F, Ahmed MH, Rasmussen EK, Petersen OS (2009) Hydrological characteristics of three north african coastal lagoons: insights from the MELMARINA project. Hydrobiologia (Incorporating JAQU) 622:45–84. https://doi.org/10.1007/s10750-008-9680-x

Topouzelis K, Spondylidis SC, Papakonstantinou A, Soulakellis N (2016) The use of Sentinel-2 imagery for seagrass mapping: Kalloni Gulf (Lesvos Island, Greece) case study. Proceedings of the Fourth International Conference on Remote Sensing and Geoinformation of the Environment, Paphos, Cyprus, 9688, pp 96881F. https://ui.adsabs.harvard.edu/link_gateway/2016SPIE.9688https://doi.org/10.1117/12.2242887

Topouzelis K, Makri D, Stoupas N, Papakonstantinou A, Katsanevakis S (2018) Seagrass mapping in greek territorial waters using Landsat-8 satellite images. International Journal of Applied Earth Observation and Geoinformation 67:98–113. https://doi.org/10.1016/j.jag.2017.12.013

Traganos D, Reinartz P (2018a) Interannual change detection of Mediterranean Seagrasses using Rapideye image time series Frontiers in Plant Science 9:96. https://doi.org/10.3389/fpls.2018.00096

Traganos D, Reinartz P (2018b) Mapping Mediterranean seagrasses with Sentinel-2 imagery. Marine Pollution Bulletin 134:197–209. https://doi.org/10.1016/j.marpolbul.2017.06.075

Trimble (2014) Ecognition developer: user guide. Trimble Germany GmbH, Munich

Villoslada M, Bergamo TF, Ward RD, Burnside NG, Joyce CB, Bunce RGH, Sepp K (2020) Fine scale plant community assessment in coastal meadows using UAV based multispectral data. Ecological Indicators 111:1–13. https://doi.org/10.1016/j.ecolind.2019.105979

Wicaksono P, Wulandari SA, Lazuardi W, Munir M (2021) Sentinel-2 images deliver possibilities for accurate and consistent multi-temporal benthic habitat maps in optically shallow water. Remote Sensing Applications: Society and Environment, 100572. https://doi.org/10.1016/j.rsase.2021.100572

Zhang C (2015) Applying data fusion techniques for benthic habitat mapping and monitoring in a coral reef ecosystem. ISPRS Journal of Photogrammetry and Remote Sensing 104:213–223. https://doi.org/10.1016/j.isprsjprs.2014.06.005

Zhang C, Selch D, Xie Z, Roberts C, Cooper H, Chen G (2013) Object-based benthic habitat mapping in the Florida Keys from hyperspectral imagery. Estuarine, Coastal and Shelf Science 134:88–97. https://doi.org/10.1016/j.ecss.2013.09.018

Zoffoli LM, Gernez P, Rosa P, le Bris A, Brando VE, Barillé A, Harin N, Peters S, Poser K, Spaias L, Peralta G, Barillé L (2020) Sentinel-2 remote sensing of Zostera noltei -dominated intertidal seagrass meadows. Remote Sensing of Environment 251:112020. https://doi.org/10.1016/j.rse.2020.112020

Zoffoli ML, Gernez P, Godet L, Peters S, Oiry S, Barillé L (2021) Decadal increase in the ecological status of a North-Atlantic intertidal seagrass meadow observed with multi-mission satellite time-series. Ecological Indicators 130:108033. https://doi.org/10.1016/j.ecolind.2021.108033

Zulkifli L, Syukur A, Patech LR (2021) Seagrass conservation needs based on the assessment of local scale economic value on the diversity of its associated biota in the South Coast East Lombok, Indonesia. Proceedings of the IOP Conf. Ser.: Earth and Environmental Science; 3rd international conference on bioscience and biotechnology Lombok, Indonesia. 712(012037). https://doi.org/10.1088/1755-1315/712/1/012037